IOPscience iopscience.iop.org

Home Search Collections Journals About Contact us My IOPscience

1/S expansion for dynamical structure factors in a two-dimensional Heisenberg antiferromagnet at zero temperature

This article has been downloaded from IOPscience. Please scroll down to see the full text article.

1992 J. Phys.: Condens. Matter 4 10265

(http://iopscience.iop.org/0953-8984/4/50/015)

View the table of contents for this issue, or go to the journal homepage for more

Download details:
IP Address: 171.66.16.96
The article was downloaded on 11/05/2010 at 01:00

Please note that terms and conditions apply.

J. Phys.: Condens. Matter 4 (1992) 10265–10276. Printed in the UK

$1/S$ expansion for dynamical structure factors in a two-dimensional Heisenberg antiferromagnet at zero temperature

Jun-ichi Igarashi

Faculty of Engineering, Gunma University, Kiryu, Gunma 376, Japan

Received 2 July 1992, in final form 29 September 1992

Abstract. We calculate the dynamical structure factors of a two-dimensional Heisenberg antiferromagnet at $T = 0$, to order $1/(2S)^2$, taking careful account of the umklapp processes. We show that, for the transverse spin part, the terms of order $1/(2S)^2$ give rise to a broad sideband peak of three-magnon excitations, whose intensity is small but not negligible. For the longitudinal spin part, the terms of order $1/(2S)^2$ modify noticeably the spectral shape of the continuum of two-magnon excitations as a function of frequency. These results could be observed in future neutron scattering experiments.

1. Introduction

There has been growing interest in quantum antiferromagnets after the discovery of high-temperature superconductors, since the undoped mother materials such as La_2CuO_4 are well described by a square-lattice spin-$\frac{1}{2}$ antiferromagnetic Heisenberg model. It is now widely accepted that this system exhibits long-range Néel order at $T = 0$, in spite of large quantum fluctuation [1–3].

Under the presence of Néel long-range order, the $1/S$ expansion may work well for treating large quantum fluctuations, where S is the magnitude of spin. Recently, the present author and Watabe [4], Castilla and Chakravarty [5], Canali, Girvin and Wallin [6] and the present author [7] have calculated several thermodynamic quantities, up to order $1/(2S)^2$. The values of order $1/(2S)^2$ are not large, indicating that the linear spin-wave (LSW) theory [8, 9] provides quite satisfactory estimates, consistent with the results given by other methods [10–13].

In this paper, we focus our attention on the dynamical structure factors, which have not yet been calculated systematically in the $1/S$ expansion. The present author and Watabe tried to calculate the dynamical structure factors in the $1/S$ expansion [4], but the treatment of the umklapp processes, which may have important contributions, was not correct. Paying careful attention on those processes in this paper, we calculate the dynamical structure factors for 'staggered' spins up to order $1/(2S)^2$, for both the transverse-spin part $S^{+-}(k, \omega)$ and the longitudinal-spin part $S^{zz}(k, \omega)$. It is shown that, for the transverse-spin part, the terms of order $1/(2S)^2$ give rise to a broad sideband peak due to three-magnon excitations in the constant-k plot, where the intensity of the sideband is one order of magnitude smaller than the intensity of the δ-function peak arising from one-magnon excitation. In the constant-ω plot of

0953-8984/92/5010265+12$07.50 © 1992 IOP Publishing Ltd

$S^{+-}(\boldsymbol{k},\omega)$, the second-order contributions give rise to a structureless feature around $\boldsymbol{k}=0$, in addition to the one-magnon peak. As for the longitudinal-spin part, the leading term is of order $1/(2S)$, where the function in the constant-k plot consists of the energy continuum of two-magnon excitations with a threshold as a function of ω, at which the intensity diverges as $\boldsymbol{k}\to 0$. The contribution of order $1/(2S)^2$ is small near the threshold frequency, but becomes considerable for large ω and $|\boldsymbol{k}|$, indicating that the convergence of the $1/S$ expansion becomes poor for larger ω and $|\boldsymbol{k}|$. In the constant-ω plot, the first-order contribution gives rise to considerable intensities around $\boldsymbol{k}=0$. The second-order contributions are found to be extremely small in this plot. Furthermore, we calculate the instantaneous spin-correlation functions. We show that they are noticeably reduced by the second-order correction. We expect that these results could be revealed by future neutron scattering experiments.

In section 2 we express the Hamiltonian in powers of $1/(2S)$ using the Holstein–Primakoff transformation. We calculate the dynamical structure factors in section 3. In section 4, we calculate the instantaneous spin-correlation functions. Section 5 is devoted to the concluding remarks.

2. Hamiltonian

We consider a square-lattice spin-$\frac{1}{2}$ antiferromagnetic Heisenberg model,

$$H = J\sum_{\langle i,j\rangle} \boldsymbol{S}_i\cdot\boldsymbol{S}_j \tag{2.1}$$

where $\langle i,j\rangle$ indicates a sum over pairs of nearest neighbours. To the spin operators $\boldsymbol{S}_i$ and $\boldsymbol{S}_j$, we apply the Holstein–Primakoff transformation [14] defined by

$$S_i^z = S - a_i^\dagger a_i \tag{2.2}$$

$$S_i^+ = (S_i^-)^\dagger = \sqrt{2S}\,f_i(S)a_i \tag{2.3}$$

$$S_j^z = -S + b_j^\dagger b_j \tag{2.4}$$

$$S_j^+ = (S_j^-)^\dagger = \sqrt{2S}\,b_j^\dagger f_j(S) \tag{2.5}$$

with

$$f_\ell(S) = (1-n_\ell/2S)^{1/2} = 1-\tfrac{1}{2}n_\ell/2S-\tfrac{1}{8}(n_\ell/2S)^2+\cdots \tag{2.6}$$

where a_i and b_j are boson annihilation operators with the indices i and j referring to sites on the a ('up') and b ('down') sublattices, respectively. The n_ℓ is $a_i^\dagger a_i$ or $b_j^\dagger b_j$. Substituting (2.2)–(2.6) into (2.1), we can expand the Hamiltonian in powers of $1/(2S)$. The terms of order $2S$ are quadratic in the boson operators, which may be diagonalized by the following Bogoliubov transformation:

$$a_{\boldsymbol{k}}^\dagger = \ell_{\boldsymbol{k}}\alpha_{\boldsymbol{k}}^\dagger + m_{\boldsymbol{k}}\beta_{-\boldsymbol{k}} \tag{2.7}$$

$$b_{-\boldsymbol{k}} = m_{\boldsymbol{k}}\alpha_{\boldsymbol{k}}^\dagger + \ell_{\boldsymbol{k}}\beta_{-\boldsymbol{k}} \tag{2.8}$$

with

$$\ell_{\boldsymbol{k}} = [(1+\epsilon_{\boldsymbol{k}})/2\epsilon_{\boldsymbol{k}}]^{1/2} \qquad m_{\boldsymbol{k}} = -[(1-\epsilon_{\boldsymbol{k}})/2\epsilon_{\boldsymbol{k}}]^{1/2} \equiv -x_{\boldsymbol{k}}\ell_{\boldsymbol{k}} \tag{2.9}$$

$$\epsilon_{\boldsymbol{k}} = (1-\gamma_{\boldsymbol{k}}^2)^{1/2} \qquad \gamma_{\boldsymbol{k}} = \cos(k_x/2)\cos(k_y/2) \tag{2.10}$$

where a_k and b_k are defined by

$$a_i = \left(\frac{2}{N}\right)^{1/2} \sum_k a_k \exp(\mathrm{i}k \cdot r_i) \qquad b_j = \left(\frac{2}{N}\right)^{1/2} \sum_k b_k \exp(\mathrm{i}k \cdot r_j) \tag{2.11}$$

with $-\pi < k_x \leqslant \pi$, $-\pi < k_y \leqslant \pi$ in units of $1/(\sqrt{2}a)$ (a is the nearest-neighbour distance). Then the Hamiltonian may be expressed in terms of the magnon operators α_k, β_k and their Hermitian conjugates:

$$H = H_0 + H_1 + H_2 + \cdots \tag{2.12}$$

with

$$H_0 = JSz \sum_k (\epsilon_k - 1) + JSz \sum_k \epsilon_k (\alpha_k{}^\dagger \alpha_k + \beta_k{}^\dagger \beta_k) \tag{2.13}$$

$$\begin{aligned} H_1 = {} & \frac{JSz}{2S} A \sum_k \epsilon_k (\alpha_k{}^\dagger \alpha_k + \beta_k{}^\dagger \beta_k) + \frac{-JSz}{2SN} \sum_{1234} \delta_G(1+2-3-4) \ell_1 \ell_2 \ell_3 \ell_4 \\ & \times \Big[\alpha_1^\dagger \alpha_2^\dagger \alpha_3 \alpha_4 B_{1234}^{(1)} + \beta_{-3}^\dagger \beta_{-4}^\dagger \beta_{-1} \beta_{-2} B_{1234}^{(2)} + 4 \alpha_1^\dagger \beta_{-4}^\dagger \beta_{-2} \alpha_3 B_{1234}^{(3)} \\ & + \big(2 \alpha_1^\dagger \beta_{-2} \alpha_3 \alpha_4 B_{1234}^{(4)} + 2 \beta_{-4}^\dagger \beta_{-1} \beta_{-2} \alpha_3 B_{1234}^{(5)} \\ & + \alpha_1^\dagger \alpha_2^\dagger \beta_{-3}^\dagger \beta_{-4}^\dagger B_{1234}^{(6)} + \mathrm{HC} \big) \Big] \end{aligned} \tag{2.14}$$

$$H_2 = \frac{JSz}{(2S)^2} \sum_k C_1(k) (\alpha_k^\dagger \alpha_k + \beta_k^\dagger \beta_k) + C_2(k) (\alpha_k^\dagger \beta_{-k}^\dagger + \beta_{-k} \alpha_k) + \cdots \tag{2.15}$$

where z ($= 4$) is the number of nearest neighbours, and $A = (2/N) \sum_k (1 - \epsilon_k) = 0.1579$. Abbreviations $a_1 = a_{k_1}, b_{-2} = b_{-k_2}$, $\gamma_{1-2} = \gamma_{k_1 - k_2}$, etc, are used. The Kronecker delta $\delta_G(1+2-3-4)$ represents the conservation of momenta within a reciprocal lattice vector G. The explicit expressions for the vertex functions $B_{1234}^{(i)}$ and the functions $C_i(k)$ are given in [7]. The first term in (2.14) comes out through the procedure of setting the products of four boson operators in a normal product form [15], while the quadratic terms in (2.15) come out through the procedure of setting the products of six boson operators in a normal-product form [4].

3. Dynamical structure factors

We consider the dynamical structure factors for the 'staggered' spins, defined by

$$S^{+-}(k,t) = \langle Q^+(k,t) [Q^+(k,0)]^\dagger \rangle \tag{3.1}$$

$$S^{zz}(k,t) = \langle Q^z(k,t) [Q^z(k,0)]^\dagger \rangle \tag{3.2}$$

where

$$Q^\lambda(k) = S_a^\lambda(k) - S_b^\lambda(k) \qquad \lambda = + \text{ or } z \tag{3.3}$$

with

$$S_{a(b)}^\lambda(k) = \left(\frac{2}{N}\right)^{1/2} \sum_{i(j)} S_{i(j)}^\lambda \exp(-\mathrm{i}k \cdot r_{i(j)}). \tag{3.4}$$

3.1. Transverse spin part

From (3.1), the Fourier transform of the transverse-spin part is given by

$$S^{+-}(\boldsymbol{k},\omega) = 2S(\ell_{\boldsymbol{k}} - m_{\boldsymbol{k}})^2(-1/\pi) \times \mathrm{Im}[F_{\alpha\alpha}(\boldsymbol{k},\omega) - F_{\alpha\beta}(\boldsymbol{k},\omega) - F_{\beta\alpha}(\boldsymbol{k},\omega) + F_{\beta\beta}(\boldsymbol{k},\omega)] \tag{3.5}$$

where

$$F_{\mu\nu}(\boldsymbol{k},\omega) = -\mathrm{i}\int_{-\infty}^{\infty} \mathrm{d}t\, \mathrm{e}^{\mathrm{i}\omega t}\langle T(Y_{\mu}^{+}(\boldsymbol{k},t)Y_{\nu}^{-}(\boldsymbol{k},0))\rangle \tag{3.6}$$

with

$$Y_{\alpha}^{+}(\boldsymbol{k}) = [Y_{\alpha}^{-}(\boldsymbol{k})]^{\dagger} = [\ell_{\boldsymbol{k}} S_{a}^{+}(\boldsymbol{k}) - m_{\boldsymbol{k}} S_{b}^{+}(\boldsymbol{k})]/(2S)^{1/2} \tag{3.7}$$

$$Y_{\beta}^{+}(\boldsymbol{k}) = [Y_{\beta}^{-}(\boldsymbol{k})]^{\dagger} = [-m_{\boldsymbol{k}} S_{a}^{+}(\boldsymbol{k}) + \ell_{\boldsymbol{k}} S_{b}^{+}(\boldsymbol{k})]/(2S)^{1/2}. \tag{3.8}$$

Here $\langle\,\rangle$ denotes the average over the ground state, and T is the time-ordering operator. Energy and frequency are measured in units of JSz in the following.

Equations (3.7) and (3.8) are expressed in terms of magnon operators after applying the Holstein–Primakoff transformation and Bogoliubov transformation:

$$Y_{\alpha}^{+}(\boldsymbol{k}) = D\alpha_{\boldsymbol{k}} - \frac{1}{2S}\frac{1}{N}\sum_{234}\delta_{\boldsymbol{G}}(\boldsymbol{k}+2-3-4)\ell_{\boldsymbol{k}}\ell_2\ell_3\ell_4 \times (M_{\boldsymbol{k}234}^{(1)}\beta_{-2}\alpha_3\alpha_4 + M_{\boldsymbol{k}234}^{(2)}\alpha_2^{\dagger}\beta_{-3}^{\dagger}\beta_{-4}^{\dagger} + \cdots) \tag{3.9}$$

$$Y_{\beta}^{+}(\boldsymbol{k}) = D\beta_{-\boldsymbol{k}}^{\dagger} - \frac{1}{2S}\frac{1}{N}\sum_{234}\delta_{\boldsymbol{G}}(\boldsymbol{k}+2-3-4)\ell_{\boldsymbol{k}}\ell_2\ell_3\ell_4\mathrm{sgn}(\gamma_{\boldsymbol{G}}) \times (M_{\boldsymbol{k}234}^{(2)}\beta_{-2}\alpha_3\alpha_4 + M_{\boldsymbol{k}234}^{(1)}\alpha_2^{\dagger}\beta_{-3}^{\dagger}\beta_{-4}^{\dagger} + \cdots) \tag{3.10}$$

where

$$M_{\boldsymbol{k}234}^{(1)} = -x_2 + \mathrm{sgn}(\gamma_{\boldsymbol{G}})x_{\boldsymbol{k}}x_3x_4 \tag{3.11}$$

$$M_{\boldsymbol{k}234}^{(2)} = x_3x_4 - \mathrm{sgn}(\gamma_{\boldsymbol{G}})x_{\boldsymbol{k}}x_2 \tag{3.12}$$

$$D = 1 - \Delta S/2S - \tfrac{1}{4}\Delta S(1+3\Delta S)/(2S)^2 \tag{3.13}$$

with $\Delta S = (1/N)\sum_{\boldsymbol{q}}(\epsilon_{\boldsymbol{q}}^{-1} - 1) = 0.19660$, and $\boldsymbol{G} = \boldsymbol{k}+2-3-4$. Substituting (3.9) and (3.10) into (3.6), and using the perturbation theory (corresponding diagrams are shown in figure 1), we calculate $F_{\mu\nu}(\boldsymbol{k},\omega)$ up to $1/(2S)^2$:

$$F_{\mu\nu}(\boldsymbol{k},\omega) = D^2G_{\mu\nu}^{0}(\boldsymbol{k},\omega) + G_{\mu\mu}^{0}(\boldsymbol{k},\omega)(2S)^{-2}\Sigma_{\mu\nu}^{(2)}(\boldsymbol{k},\omega)G_{\nu\nu}^{0}(\boldsymbol{k},\omega) + I_{\mu\nu}(\boldsymbol{k},\omega)G_{\nu\nu}^{0}(\boldsymbol{k},\omega) + G_{\mu\mu}^{0}(\boldsymbol{k},\omega)\bar{I}_{\mu\nu}(\boldsymbol{k},\omega) + J_{\mu\nu}(\boldsymbol{k},\omega) \tag{3.14}$$

where the $G_{\mu\nu}^{0}(\boldsymbol{k},\omega)$ are the unperturbed propagators,

$$G_{\alpha\alpha}^{0}(\boldsymbol{k},\omega) = [\omega - \epsilon_{\boldsymbol{k}} + \mathrm{i}\delta]^{-1} \tag{3.15}$$

$$G_{\alpha\beta}^{0}(\boldsymbol{k},\omega) = G_{\beta\alpha}^{0}(\boldsymbol{k},\omega) = 0 \tag{3.16}$$

$$G_{\beta\beta}^{0}(\boldsymbol{k},\omega) = [-\omega - \epsilon_{\boldsymbol{k}} + \mathrm{i}\delta]^{-1} \qquad \delta \to 0^{+} \tag{3.17}$$

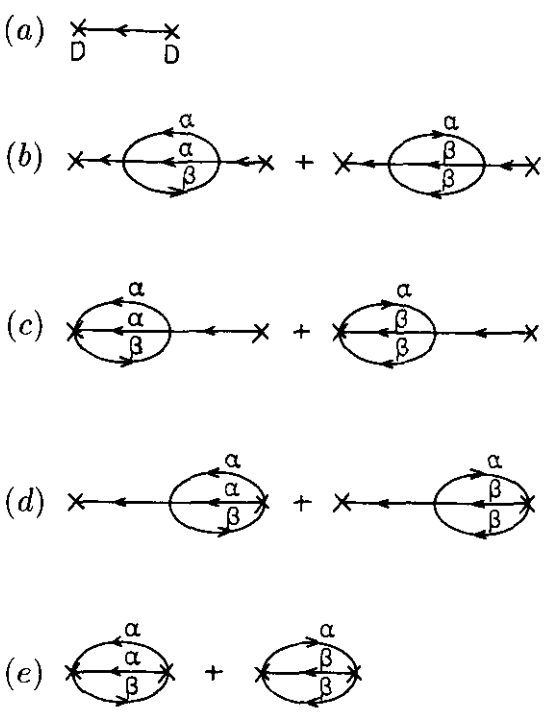

Figure 1. Diagrams for $F^{+-}_{\mu\nu}(\boldsymbol{k},\omega)$: $(a)D^2G^0_{\mu\mu}(\boldsymbol{k},\omega)$; $(b)G^0_{\mu\mu}(\boldsymbol{k},\omega)\Sigma^{(2)}_{\mu\nu}(\boldsymbol{k},\omega)G^0_{\nu\nu}(\boldsymbol{k},\omega)$; $(c)I_{\mu\nu}(\boldsymbol{k},\omega)G^0_{\nu\nu}(\boldsymbol{k},\omega)$; $(d)G^0_{\mu\mu}(\boldsymbol{k},\omega)\tilde{I}_{\mu\nu}(\boldsymbol{k},\omega)$; $(e)J_{\mu\nu}(\boldsymbol{k},\omega)$. The solid lines represent the unperturbed propagators. The crosses for (a) represent D, while the crosses for (c) and (d) represent 1 or $-\ell_{\boldsymbol{k}}\ell_{\boldsymbol{p}}\ell_{\boldsymbol{q}}\ell_{\boldsymbol{k}+\boldsymbol{p}-\boldsymbol{q}}M^{(1)}_{\boldsymbol{k},\boldsymbol{p},\boldsymbol{q},[\boldsymbol{k}+\boldsymbol{p}-\boldsymbol{q}]}/(2S)$ or $-\ell_{\boldsymbol{k}}\ell_{\boldsymbol{p}}\ell_{\boldsymbol{q}}\ell_{\boldsymbol{k}+\boldsymbol{p}-\boldsymbol{q}}\,\mathrm{sgn}(\gamma_{\boldsymbol{G}})\times M^{(2)}_{\boldsymbol{k},\boldsymbol{p},\boldsymbol{q},[\boldsymbol{k}+\boldsymbol{p}-\boldsymbol{q}]}/(2S)$ with $[\boldsymbol{k}+\boldsymbol{p}-\boldsymbol{q}]$ being the reduced value of $\boldsymbol{k}+\boldsymbol{p}-\boldsymbol{q}$ in the first Brillouin zone by a reciprocal vector $\boldsymbol{G}$.

and the self-energy parts $\Sigma^{(2)}_{\mu\nu}(\boldsymbol{k},\omega)$ are given by

$$\Sigma^{(2)}_{\alpha\alpha}(\boldsymbol{k},\omega)=\Sigma^{(2)}_{\beta\beta}(-\boldsymbol{k},-\omega)=C_1(\boldsymbol{k})+\left(\frac{2}{N}\right)^2\sum_{\boldsymbol{p}\boldsymbol{q}}2\ell^2_{\boldsymbol{k}}\ell^2_{\boldsymbol{p}}\ell^2_{\boldsymbol{q}}\ell^2_{\boldsymbol{k}+\boldsymbol{p}-\boldsymbol{q}}$$
$$\times\left[\frac{|\,B^{(4)}_{\boldsymbol{k},\boldsymbol{p},\boldsymbol{q},[\boldsymbol{k}+\boldsymbol{p}-\boldsymbol{q}]}\,|^2}{\omega-\epsilon_{\boldsymbol{p}}-\epsilon_{\boldsymbol{q}}-\epsilon_{\boldsymbol{k}+\boldsymbol{p}-\boldsymbol{q}}+\mathrm{i}\delta}-\frac{|\,B^{(6)}_{\boldsymbol{k},\boldsymbol{p},\boldsymbol{q},[\boldsymbol{k}+\boldsymbol{p}-\boldsymbol{q}]}\,|^2}{\omega+\epsilon_{\boldsymbol{p}}+\epsilon_{\boldsymbol{q}}+\epsilon_{\boldsymbol{k}+\boldsymbol{p}-\boldsymbol{q}}-\mathrm{i}\delta}\right] \tag{3.18}$$

$$\Sigma^{(2)}_{\alpha\beta}(\boldsymbol{k},\omega)=\Sigma^{(2)}_{\beta\alpha}(-\boldsymbol{k},-\omega)=C_2(\boldsymbol{k})+\left(\frac{2}{N}\right)^2\sum_{\boldsymbol{p}\boldsymbol{q}}2\ell^2_{\boldsymbol{k}}\ell^2_{\boldsymbol{p}}\ell^2_{\boldsymbol{q}}\ell^2_{\boldsymbol{k}+\boldsymbol{p}-\boldsymbol{q}}\mathrm{sgn}(\gamma_{\boldsymbol{G}})$$
$$\times B^{(4)}_{\boldsymbol{k},\boldsymbol{p},\boldsymbol{q},[\boldsymbol{k}+\boldsymbol{p}-\boldsymbol{q}]}B^{(6)}_{\boldsymbol{k},\boldsymbol{p},\boldsymbol{q},[\boldsymbol{k}+\boldsymbol{p}-\boldsymbol{q}]}\frac{2(\epsilon_{\boldsymbol{p}}+\epsilon_{\boldsymbol{q}}+\epsilon_{\boldsymbol{k}+\boldsymbol{p}-\boldsymbol{q}})}{\omega^2-(\epsilon_{\boldsymbol{p}}+\epsilon_{\boldsymbol{q}}+\epsilon_{\boldsymbol{k}+\boldsymbol{p}-\boldsymbol{q}})^2+\mathrm{i}\delta}. \tag{3.19}$$

The functions $I_{\mu\nu}(\boldsymbol{k},\omega)$, $\tilde{I}_{\mu\nu}(\boldsymbol{k},\omega)$ and $J_{\mu\nu}(\boldsymbol{k},\omega)$ correspond to figures 1(c), (d) and (e), respectively, and their explicit expressions are given in [7].

Equation (3.14) is inserted into (3.5) to obtain $S^{+-}(\boldsymbol{k},\omega)$. Apart from the energy shift, it may be expressed as

$$S^{+-}(\boldsymbol{k},\omega)=\rho_1(\boldsymbol{k})\delta(\omega-\epsilon_{\boldsymbol{k}})+\rho_2(\boldsymbol{k},\omega) \tag{3.20}$$

where

$$\rho_1(k) = 2S(\ell_k - m_k)^2\Bigg(1 - \frac{2\Delta S}{2S} + \frac{1}{(2S)^2}\Bigg\{-\tfrac{1}{2}\Delta S(1+\Delta S) + \frac{1}{\epsilon_k}\Sigma^{(2)}_{\alpha\beta}(k,\epsilon_k) + \left(\frac{2}{N}\right)^2 \sum_{pq} 2\ell_k^2\ell_p^2\ell_q^2\ell_{k+p-q}^2 \times \Bigg[\frac{-|B^{(4)}_{k,p,q,[k+p-q]}|^2}{(\epsilon_k - \epsilon_p - \epsilon_q - \epsilon_{k+p-q})^2} + \frac{|B^{(6)}_{k,p,q,[k+p-q]}|^2}{(\epsilon_k + \epsilon_p + \epsilon_q + \epsilon_{k+p-q})^2} + (M^{(1)}_{k,p,q,[k+p-q]} - \mathrm{sgn}(\gamma_G)M^{(2)}_{k,p,q,[k+p-q]}) \times \left(\frac{B^{(4)}_{k,p,q,[k+p-q]}}{\epsilon_k - \epsilon_p - \epsilon_q - \epsilon_{k+p-q}} + \frac{\mathrm{sgn}(\gamma_G)B^{(6)}_{k,p,q,[k+p-q]}}{\epsilon_k + \epsilon_p + \epsilon_q + \epsilon_{k+p-q}}\right)\Bigg]\Bigg\}\Bigg) \tag{3.21}$$

$$\rho_2(k,\omega) = 2S(\ell_k - m_k)^2\frac{1}{(2S)^2}\left(\frac{2}{N}\right)^2\sum_{pq}\delta(\omega - \epsilon_p - \epsilon_q - \epsilon_{k+p-q})\ell_k^2\ell_p^2\ell_q^2\ell_{k+p-q}^2 \times \tfrac{1}{2}\Bigg[2\Big(\frac{-B^{(4)}_{k,p,q,[k+p-q]}}{\epsilon_k - \epsilon_p - \epsilon_q - \epsilon_{k+p-q}} + \frac{\mathrm{sgn}(\gamma_G)B^{(6)}_{k,p,q,[k+p-q]}}{\epsilon_k + \epsilon_p + \epsilon_q + \epsilon_{k+p-q}}\Big) + M^{(1)}_{k,p,q,[k+p-q]} - \mathrm{sgn}(\gamma_G)M^{(2)}_{k,p,q,[k+p-q]}\Bigg]^2. \tag{3.22}$$

Here $[k+p-q]$ denotes the reduced value of $k+p-q$ in the first Brillouin zone by a reciprocal vector G. The $\rho_1(k)$ diverges as $1/\epsilon_k$ with $k \to 0$, due to the divergence of the prefactor $2S(\ell_k - m_k)^2$. On the other hand, $\rho_2(k, \omega \geqslant \epsilon_k)$ remains finite with $k \to 0$, since the divergence of the factor $(\ell_k - m_k)^2\ell_k^2$ is compensated by the terms $B^{(4)}_{k,p,q,[k+p-q]} + \mathrm{sgn}(\gamma_G)B^{(6)}_{k,p,q,[k+p-q]}[\propto \epsilon_k]$ and $M^{(1)}_{k,p,q,[k+p-q]} - \mathrm{sgn}(\gamma_G)M^{(2)}_{k,p,q,[k+p-q]}[\propto \epsilon_k]$.

We evaluate (3.21) and (3.22) by summing 25600 points of p and q in the first Brillouin zone. Figure 2 shows $S^{+-}(k,\omega)$ for $S = \frac{1}{2}$ with $k = (17\pi/160, 17\pi/160)$ and $k = (129\pi/160, 129\pi/160)$, as a function of ω (constant-k plot). There appears a broad sideband peak of three-magnon excitations, in addition to the δ-function of one-magnon excitation. Figure 3 shows $S^{+-}(k,\omega)$ for $S = \frac{1}{2}$ with $\omega = 0.2333$, as a function of k along a line of $k_x = k_y$ (constant-ω plot). The intensities around $k = 0$, which arise from three-magnon excitations ($\rho_2(k,\omega)$), are structureless and weak.

3.2. Longitudinal spin part

Applying the Bogoliubov transformation to (2.2) and (2.4), we may express the z-component of 'staggered' spin as

$$Q^z(k) = 2(S - \Delta S)(N/2)^{1/2}\delta(k) + R(k) \tag{3.23}$$

with

$$R(k) = -\left(\frac{2}{N}\right)^{1/2}\sum_p \ell_p\ell_{p+k}[(1 + x_px_{p+k})(\alpha_p^\dagger\alpha_{p+k} + \beta^\dagger_{-p-k}\beta_{-p}) - (x_p + x_{p+k})(\alpha_p^\dagger\beta^\dagger_{-p-k} + \beta_{-p}\alpha_{p+k})]. \tag{3.24}$$

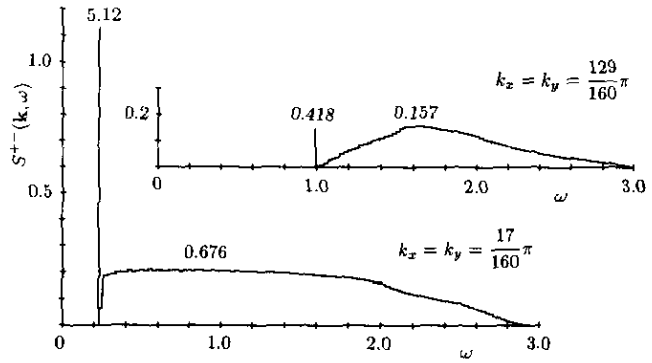

Figure 2. Dynamical structure factors for the transverse-spin part $S^{+-}(\boldsymbol{k},\omega)$ with $\boldsymbol{k} = (17\pi/160,\ 17\pi/160)$ and with $\boldsymbol{k} = (129\pi/160,\ 129\pi/160)$, as a function of ω (constant-$\boldsymbol{k}$ plot). $S = \frac{1}{2}$. The straight vertical lines represent the δ-functions, whose intensities are given by the attached numbers ($\rho_1(\boldsymbol{k})$). The histograms represent the sideband spectra $\rho_2(\boldsymbol{k},\omega)$. The intensities integrated over ω are given by the numbers attached to the histograms.

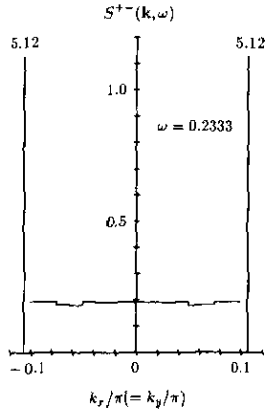

Figure 3. Dynamical structure factors for the transverse-spin part $S^{+-}(\boldsymbol{k},\omega)$ with $\omega = 0.2333$, as a function of $\boldsymbol{k}$ along a line of $k_x = k_y$ (constant-ω plot). $S = \frac{1}{2}$. The straight vertical lines represent the δ-functions, whose intensities are given by the attached numbers [$\rho_1(\pm\boldsymbol{k}_0)$ for $\boldsymbol{k}_0 = (17\pi/160,\ 17\pi/160)$]. The histograms represent $\rho_2(\boldsymbol{k}, \omega = 0.2333)$.

Substituting (3.23) into (3.2), we may express the dynamical structure factor as

$$S^{zz}(\boldsymbol{k},\omega) = 2(S - \Delta S)^2 N\delta(\boldsymbol{k})\delta(\omega) + S^{zz}_{\text{inc}}(\boldsymbol{k},\omega) \tag{3.25}$$

where

$$S^{zz}_{\text{inc}}(\boldsymbol{k},\omega) = \frac{2}{N}\sum_{\boldsymbol{p}\boldsymbol{p}'}\delta(\omega - \epsilon_{\boldsymbol{p}} - \epsilon_{\boldsymbol{p}+\boldsymbol{k}})\ell_{\boldsymbol{p}}\ell_{\boldsymbol{p}+\boldsymbol{k}}\ell_{\boldsymbol{p}'}\ell_{\boldsymbol{p}'+\boldsymbol{k}}(x_{\boldsymbol{p}} + x_{\boldsymbol{p}+\boldsymbol{k}})(x_{\boldsymbol{p}'} + x_{\boldsymbol{p}'+\boldsymbol{k}})$$
$$\times\left(-\frac{1}{\pi}\right)\text{Im}\left[\sum_{mn} W_{m\boldsymbol{p},n\boldsymbol{p}'}(\boldsymbol{k},\omega)\right] + \cdots \tag{3.26}$$

with

$$W_{1\boldsymbol{p},1\boldsymbol{p}'}(\boldsymbol{k},\omega) = -\mathrm{i}\int_{-\infty}^{\infty} \mathrm{d}t\, \mathrm{e}^{\mathrm{i}\omega t}\langle T[\beta_{-\boldsymbol{p}}(t)\alpha_{\boldsymbol{p}+\boldsymbol{k}}(t)\alpha^{\dagger}_{\boldsymbol{p}'+\boldsymbol{k}}(0)\beta^{\dagger}_{-\boldsymbol{p}'}(0)]\rangle \tag{3.27}$$

$$W_{1\boldsymbol{p},2\boldsymbol{p}'}(\boldsymbol{k},\omega) = -\mathrm{i}\int_{-\infty}^{\infty} \mathrm{d}t\, \mathrm{e}^{\mathrm{i}\omega t}\langle T[\beta_{-\boldsymbol{p}}(t)\alpha_{\boldsymbol{p}+\boldsymbol{k}}(t)\beta_{-\boldsymbol{p}'-\boldsymbol{k}}(0)\alpha_{\boldsymbol{p}'}(0)]\rangle \tag{3.28}$$

$$W_{2\boldsymbol{p},1\boldsymbol{p}'}(\boldsymbol{k},\omega) = -\mathrm{i}\int_{-\infty}^{\infty} \mathrm{d}t\, \mathrm{e}^{\mathrm{i}\omega t}\langle T[\alpha^{\dagger}_{\boldsymbol{p}}(t)\beta^{\dagger}_{-\boldsymbol{p}-\boldsymbol{k}}(t)\alpha^{\dagger}_{\boldsymbol{p}'+\boldsymbol{k}}(0)\beta^{\dagger}_{-\boldsymbol{p}'}(0)]\rangle \tag{3.29}$$

$$W_{2\boldsymbol{p},2\boldsymbol{p}'}(\boldsymbol{k},\omega) = -\mathrm{i}\int_{-\infty}^{\infty} \mathrm{d}t\, \mathrm{e}^{\mathrm{i}\omega t}\langle T[\alpha^{\dagger}_{\boldsymbol{p}}(t)\beta^{\dagger}_{-\boldsymbol{p}-\boldsymbol{k}}(t)\beta_{-\boldsymbol{p}'-\boldsymbol{k}}(0)\alpha_{\boldsymbol{p}'}(0)]\rangle. \tag{3.30}$$

The first term of (3.25) represents the magnetic Bragg scattering arising from the antiferromagnetic long-range order, while $S^{zz}_{\mathrm{inc}}(\boldsymbol{k},\omega)$ describes the inelastic scattering.

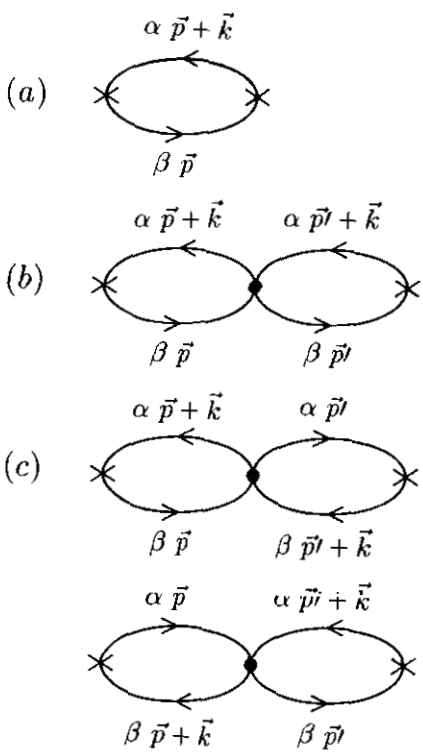

Figure 4. Diagrams for $W(\boldsymbol{k},\omega)$: (*a*) the lowest-order diagrams to $W_{1\boldsymbol{p},1\boldsymbol{p}}(\boldsymbol{k},\omega)$; (*b*) the next-order diagram to $W_{1\boldsymbol{p},1\boldsymbol{p}'}(\boldsymbol{k},\omega)$; (*c*) the next-order diagrams to $W_{1\boldsymbol{p},2\boldsymbol{p}'}(\boldsymbol{k},\omega)$ and $W_{2\boldsymbol{p},1\boldsymbol{p}'}(\boldsymbol{k},\omega)$. The solid lines with μ $\boldsymbol{p}$ and μ $\boldsymbol{p}+\boldsymbol{k}$ represent the unperturbed Green's functions $G^0_{\mu\mu}(\boldsymbol{p},\omega')$ and $G^0_{\mu\mu}(\boldsymbol{p}+\boldsymbol{k},\omega'+\omega)$, respectively. The solid circles represent the interaction between magnons given by H_1.

The perturbation theory is used to calculate $W(\boldsymbol{k},\omega)$. For the lowest-order diagram (figure 4(*a*)), we have

$$-(1/\pi)\mathrm{Im}\ W_{1\boldsymbol{p},1\boldsymbol{p}}(\boldsymbol{k},\omega) = \delta(\omega-\epsilon_{\boldsymbol{p}}-\epsilon_{\boldsymbol{p}+\boldsymbol{k}}) \qquad \text{for} \quad \omega > 0. \tag{3.31}$$

The other components are zero in this order. For the next-order diagrams (figure 4(*b*) and (*c*)), we find

$$-(1/\pi)\mathrm{Im}\ W_{1\boldsymbol{p},1\boldsymbol{p}'}(\boldsymbol{k},\omega)[\delta(\omega-\epsilon_{\boldsymbol{p}}-\epsilon_{\boldsymbol{p}+\boldsymbol{k}})-\delta(\omega-\epsilon_{\boldsymbol{p}'}-\epsilon_{\boldsymbol{p}'+\boldsymbol{k}})] \times V_{1\boldsymbol{p},1\boldsymbol{p}'}(\boldsymbol{k})/(\epsilon_{\boldsymbol{p}}+\epsilon_{\boldsymbol{p}+\boldsymbol{k}}-\epsilon_{\boldsymbol{p}'}-\epsilon_{\boldsymbol{p}'+\boldsymbol{k}}) \tag{3.32}$$

$$-(1/\pi)\mathrm{Im}\ W_{1\boldsymbol{p},2\boldsymbol{p}'}(\boldsymbol{k},\omega) = -(1/\pi)\mathrm{Im}\ W_{2\boldsymbol{p}',1\boldsymbol{p}}(\boldsymbol{k},\omega) = -\delta(\omega-\epsilon_{\boldsymbol{p}}-\epsilon_{\boldsymbol{p}+\boldsymbol{k}})V_{1\boldsymbol{p},2\boldsymbol{p}'}(\boldsymbol{k})/(\epsilon_{\boldsymbol{p}}+\epsilon_{\boldsymbol{p}+\boldsymbol{k}}+\epsilon_{\boldsymbol{p}'}+\epsilon_{\boldsymbol{p}'+\boldsymbol{k}}) \tag{3.33}$$

with

$$V_{1p,1p'}(k) = V_{2p,2p'}(k) = -(1/N)(1/2S)4\ell_{p+k}\ell_{p'}\ell_{p'+k}\ell_p B^{(3)}_{[p+k],p',[p'+k],p} \tag{3.34}$$

$$V_{1p,2p'}(k) = V_{2p,1p'}(k) = -(1/N)(1/2S)4\ell_{p+k}\ell_{p'}\ell_{p'+k}\ell_p B^{(6)}_{[p+k],p',[p'+k],p} \tag{3.35}$$

with $[p+k]$ denoting the reduced value of $p+k$ in the first Brillouin zone. From (3.31)–(3.33), we obtain

$$\begin{aligned} S^{zz}_{\rm inc}(k,\omega) = \frac{2}{N}\sum_{pp'}\delta(\omega-\epsilon_p-\epsilon_{p+k})\ell_p\ell_{p+k}\ell_{p'}\ell_{p'+k}(x_p+x_{p+k})(x_{p'}+x_{p'+k}) \\ \times\Big[\delta(p-p')+2V_{1p,1p'}(k)/(\epsilon_p+\epsilon_{p+k}-\epsilon_{p'}-\epsilon_{p'+k}) \\ -2V_{1p,2p'}(k)/(\epsilon_p+\epsilon_{p+k}+\epsilon_{p'}+\epsilon_{p'+k})\Big]. \end{aligned} \tag{3.36}$$

In the last factor of (3.36), the first term may be called the first-order contribution, and the second and the third terms may be called the second-order contribution, since they correspond to the corrections of order $1/(2S)$ and of order $1/(2S)^2$ to $S^{zz}(k,\omega)$, respectively. The sum over p' for the second term is performed in such a way as to give Cauchy's principal value. Note that $S^{zz}_{\rm inc}(k,\omega)$ is non-zero only for $\omega \geqslant \epsilon_k$, and increases as $1/\mid k \mid$ with $\mid k \mid \to 0$ for ω close to the threshold energy ϵ_k.

We evaluate (3.36) by summing 25600 points of p and p' in the first Brillouin zone. Figure 5 shows $S^{zz}(k,\omega)$ thus evaluated for $S=\frac{1}{2}$ with $k=(17\pi/160, 17\pi/160)$ and $k=(129\pi/160, 129\pi/160)$, as a function of ω (constant-k plot). The first-order contribution is dominant for small $\mid k \mid$, and its integrated intensity decreases with increasing $\mid k \mid$ and ω. The second-order correction, which is negative, becomes important for large $\mid k \mid$ and ω, indicating that the the convergence of the $1/S$ expansion becomes poor in this region. Figure 6 shows $S^{zz}(k,\omega)$ for $S=\frac{1}{2}$ with $\omega = 0.2333$ as a function of k along a line of $k_x = k_y$ (constant-ω plot). There appears considerable intensity around $k=0$. This arises from the first-order contribution, while the second-order contribution is very small around $k=0$, due to a partial cancellation between the second and third terms in the last factor of (3.36).

4. Instantaneous spin-correlation functions

The instantaneous spin-correlation functions are calculated by integrating the dynamical structure factors with respect to frequency ω:

$$S^{+-}(k) \equiv \langle Q^+(k)[Q^+(k)]^\dagger\rangle = \rho_1(k) + \int_{-\infty}^{\infty} {\rm d}\omega\ \rho_2(k,\omega) \tag{4.1}$$

$$\begin{aligned} S^{zz}(k) \equiv \langle Q^z(k)[Q^z(k)]^\dagger\rangle = 2(S-\Delta S)^2 N\delta(k) \\ + \frac{2}{N}\sum_{pp'}\ell_p\ell_{p+k}\ell_{p'}\ell_{p'+k}(x_p+x_{p+k})(x_{p'}+x_{p'+k}) \\ \times\Big[\delta(p-p') - 2V_{1p,2p'}(k)/(\epsilon_p+\epsilon_{p+k}+\epsilon_{p'}+\epsilon_{p'+k})\Big]. \end{aligned} \tag{4.2}$$

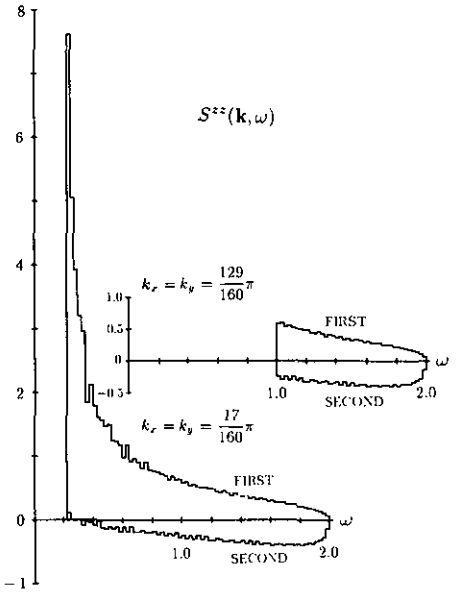

Figure 5. Dynamical structure factors for the longitudinal-spin part $S^{zz}(\boldsymbol{k},\omega)$ with $\boldsymbol{k} = (17\pi/160,\ 17\pi/160)$ and with $\boldsymbol{k} = (129\pi/160,\ 129\pi/160)$, as a function of ω (constant-k plot). $S = \frac{1}{2}$. The histograms with letters 'FIRST' represent the first-order contributions, while the histograms with letters 'SECOND' represent the second-order contributions.

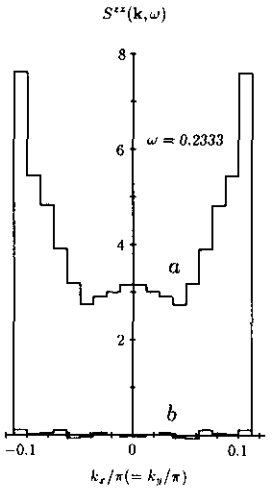

Figure 6. Dynamical structure factors for the longitudinal-spin part $S^{zz}(\boldsymbol{k},\omega)$ with $\omega = 0.2333$, as a function of $\boldsymbol{k}$ along a line of $k_x = k_y$ (constant-ω plot). $S = \frac{1}{2}$. Histograms a and b represent the first-order and the second-order contributions, respectively.

The explicit expression for the last term in (4.1) is given by geting rid of the factor $\delta(\omega - \epsilon_{\boldsymbol{p}} - \epsilon_{\boldsymbol{q}} - \epsilon_{\boldsymbol{k}+\boldsymbol{p}-\boldsymbol{q}})$ from (3.22). We evaluate (4.1) and (4.2) by summing 6400 points of $\boldsymbol{p}$ and $\boldsymbol{p}'$ in the first Brillouin zone. Figure 7 shows $S^{+-}(\boldsymbol{k})$ and $S^{zz}(\boldsymbol{k})$ thus evaluated for $S = \frac{1}{2}$: curves a and b represent $S^{+-}(\boldsymbol{k})$ in lowest order and up to second order in $1/(2S)$, respectively, while curves c and d represent $S^{zz}(\boldsymbol{k})$ evaluated to first order and up to second order in $1/(2S)$, respectively. Note that the spin correlations are suppressed by the second-order corrections in both the transverse and longitudinal-spin parts. Figure 8 shows the spherically averaged spin-correlation function $S(\boldsymbol{k})$ $[\equiv S^{+-}(\boldsymbol{k}) + S^{zz}(\boldsymbol{k})]$ for $S = \frac{1}{2}$. To lowest order in $1/(2S)$, $S(\boldsymbol{k})$ is given by the LSW value, i.e., $2S(\ell_{\boldsymbol{k}} - m_{\boldsymbol{k}})^2$ when $|\boldsymbol{k}| \neq 0$. Up to order $1/(2S)^2$, the value remains very close to the LSW values, since the reduction caused by the second-order correction in $S^{+-}(\boldsymbol{k})$ is mostly compensated by $S^{zz}(\boldsymbol{k})$. This result is consistent with the calculations by the variational method and by exact diagonalization for finite clusters, which gives values very close to the LSW theory [12].

5. Concluding remarks

We have calculated the dynamical structure factors up to order $1/(2S)^2$ in the $1/S$ expansion, by using the Holstein–Primakoff transformation. The contributions of order $1/(2S)^2$ are found, on the whole, not to be large, indicating that the $1/S$ expansion is a good asymptotic expansion for dynamical quantities. This result

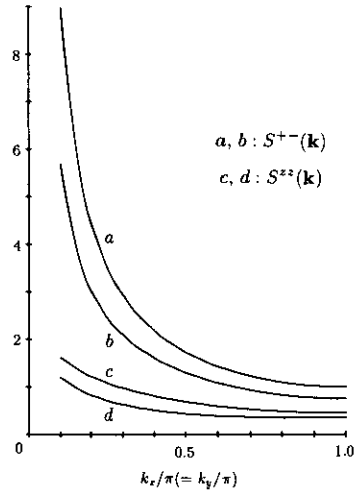

Figure 7. Instantaneous spin-correlation functions. Curves a and b represent the lowest-order values and the values up to order $1/(2S)^2$ for $S^{+-}(\boldsymbol{k})$. Curves c and d represent the first-order value and the values up to order $1/(2S)^2$ for $S^{zz}(\boldsymbol{k})$, respectively.

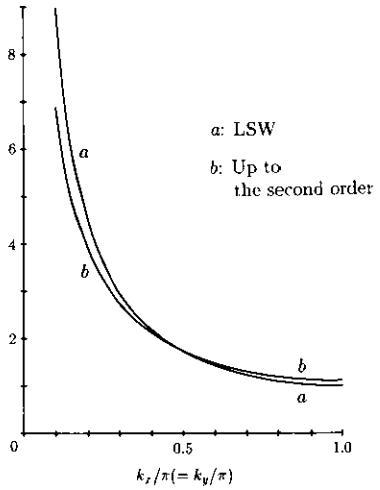

Figure 8. Instantaneous spin-correlation function for the spherically-averaged part $S(\boldsymbol{k}) = S^{+-}(\boldsymbol{k}) + S^{zz}(\boldsymbol{k})$. Curve a represents the lowest-order values, and curve b represents the values summed to order $1/(2S)^2$.

is consistent with the fact that the contributions of order $1/(2S)^2$ are small for thermodynamic quantities [4–7]. Although its intensity is not large, a broad peak of sideband was found in $S^{+-}(k, \omega)$. This arises from non-linearity of the second-order contributions. Such a non-linear effect might be responsible for the high-frequency tail found in two-magnon Raman-scattering spectra in La_2CuO_4 [16]. For $S^{zz}(k, \omega)$, the leading term is of order $1/(2S)$, which gave the spectral shape composed of the energy continuum of two-magnon excitations as a function of frequency. The shape was found to be noticeably modified by the magnon–magnon scattering in the second-order contributions. We expect that the deviation from the LSW values could be observed by future neutron scattering experiments.

We have also calculated the instantaneous spin-correlation functions. We found again that the leading-order contributions in both the transverse and the longitudinal spin parts are considerably reduced by the second-order contributions. On the other hand, as already pointed out by the present author and Watabe [4], when the functions are averaged over the spin directions for $S = \frac{1}{2}$, the second-order correction to $S^{+-}(k)$ are nearly cancelled out by $S^{zz}(k)$, making the averaged values very close to the LSW values, consistent with Monte Carlo calculations [2] and exact diagonalization for finite clusters [12]. If the transverse and the longitudinal components are separately measured, the deviations from the LSW values could be observed.

Acknowledgments

The author would like to thank H Akai, S Honma and S Miyazawa for valuable

discussions. This work was partially supported by a Grant-in-Aid for Scientific Research from the Japanese Ministry of Education, Science and Culture.

References

[1] Reger J D and Young A P 1988 *Phys. Rev.* B **37** 5978
[2] Miyashita S 1988 *J. Phys. Soc. Japan* **57** 1934
Okabe Y and Kikuchi M 1988 *J. Phys. Soc. Japan* **57** 4351
[3] Chakravarty S, Halperin B I and Nelson D R 1988 *Phys. Rev. Lett.* **60** 1057; 1989 *Phys. Rev.* B **39** 2344
[4] Igarashi J and Watabe A 1991 *Phys. Rev.* B **43** 13456; **44** 5057
[5] Castilla G E and Chakravarty S 1991 *Phys. Rev.* B **43** 13687
[6] Canali C M, Girvin S M and Wallin M 1992 *Phys. Rev.* B **45** 10131
[7] Igarashi J 1992 *Phys. Rev.* B **46** 10736
[8] Anderson P W 1952 *Phys. Rev.* **86** 694
[9] Kubo R 1952 *Phys. Rev.* **87** 568
[10] Singh R R P 1989 *Phys. Rev.* B **39** 9760
Singh R R P and Huse D A 1989 *Phys. Rev.* B **40** 7247
[11] Trivedi N and Ceperley D M 1989 *Phys. Rev.* B **40** 2737
[12] Horsch P and von der Linden W 1988 *Z. Phys* B **72** 181
[13] Becker K W, Won H and Fulde P 1989 *Z. Phys* B **75** 335
[14] Holstein T and Primakoff H 1940 *Phys. Rev.* **58** 1098
[15] Oguchi T 1960 *Phys. Rev.* **117** 117
[16] Sugai S 1990 *Solid State Commun.* **75** 795